



Thermally induced irreversibility in the conductivity of germanium nitride and oxynitride films



N. Pinto^{a,b,*}, F. Caproli^a, G. Maggioni^c, S. Carturan^c, D.R. Napoli^d

^a Scuola di Scienze e Tecnologie, sezione di Fisica, Università di Camerino, Camerino, Italy

^b INFN, sezione di Perugia, Perugia, Italy

^c INFN, Laboratori Nazionali di Legnaro, Legnaro, PD, Italy

^d Dipartimento di Fisica e Astronomia, Università di Padova, Padova, Italy

ARTICLE INFO

Keywords:

Germanium nitride
Germanium oxynitride
Thermal annealing
Electrical conductivity

ABSTRACT

We report the evidence for irreversible changes in the conductivity, $\sigma(T)$, of a-Ge₃N_x ($3.7 < x < 4.6$) and quasi-stoichiometric a-Ge₂O_yN_x thin films occurring at $T \gtrsim 630$ K, under high vacuum conditions. We have found that $\sigma(T)$ curves not only depend on the material properties but also on the thermal history undertaken by films. The irreversibility in $\sigma(T)$, during heating in vacuum, is correlated to the transformation of the native GeO₂ into volatile GeO. Thermal annealing in N₂ atmosphere, on the contrary, results to extend film stability up to 973 K. At higher T , domes and pits are formed onto the film surface, due to the strong effusion of N-rich volatile species. Unstable N-Ge bonds can explain both the nitrogen thermodynamic instability and the Ge nano-crystallisation process occurring in a-Ge₃N_x films, upon heating until 1023 K. Compared to a-Ge₃N_x, quasi-stoichiometric a-Ge₂O_yN_x is both more insulating and more stable upon heating up to 1023 K under N₂ flow, that makes it a suitable passivating layer material for the fabrication of electronic devices.

1. Introduction

Germanium based nitrides and oxynitrides, both in crystalline and amorphous phases, are dielectric materials interesting for several technological applications [1,2]. With respect to GeO_x native oxide, composed of the unstable GeO and hydrosoluble GeO₂ [3,4], GeN as well as GeON alloys can compete with the high stability, ease of formation and thickness control of SiO₂ for Si based devices [1]. Germanium nitride and/or oxynitride have been tested to be good candidates as dielectric layer for phase change memory [2,5] and as gate interlayer for capacitors and transistors fabrication as well [6]. Ge₃N₄, with a band gap of ≈ 4.5 eV, is a good candidate as a passivating layer for metal oxide semiconductor capacitors [7] and for the fabrication of high performance and low leakage current Ge *p-n* junctions as well [8]. This last kind of application has been pushing forward with research activity to develop high performance γ -ray detectors based on high purity Ge crystals (HPGe) [9].

Despite interesting potential applications, the electrical properties of GeN and GeON based dielectric alloys are only partially known since the huge insulating properties of this class of materials represents an obstacle to carry out reliable measurements.

Data reported in literature refer to under-stoichiometric a-GeN alloys, both H-free and hydrogenated, as well as nitrogen doped c-Ge and

a-Ge [10]. For these systems, experiments have demonstrated that insulating properties of both Ge₃N_x and Si₃N_x deteriorate notably as the nitrogen concentration decreases far below $x \approx 4$ [10].

In previous studies carried out on this class of materials, the authors investigated the properties of the as-deposited films and their electronic transport properties, aimed to find the optimal deposition parameters to fabricate thin layers having the best insulating properties. The effects of the deposition parameters on the electrical properties were also studied in a temperature range from R.T. up to 600 K [11,12].

We have extended the investigation to the thermal stability of a-Ge₃N_x and a-Ge₂O_yN_x films upon high temperature annealing under a N₂ gas flow. Composition, structure, morphology and conductivity have been extensively studied in annealed samples. Compared to the other techniques used in this study, we have found that the electrical conductivity is very sensitive in detecting thermally-induced irreversible changes occurring during the measurements. The results obtained by the electrical characterisation of as-deposited films (Section 3.1) extend previous studies the reader is referred to [11,12].

2. Experimental

Thin films of a-Ge₃N_x and a-Ge₂O_yN_x were deposited at room temperature (R.T.), by reactive r.f. magnetron sputtering. Deposition was

* Corresponding author at: Scuola di Scienze e Tecnologie, sezione di Fisica, Università di Camerino, Camerino, Italy.
E-mail address: nicola.pinto@unicam.it (N. Pinto).

Table 1

Properties of a-Ge₃N_x and a-Ge₂O_yN_x films deposited under different conditions. From left to right: sample name; as-deposited film stoichiometry measured by the RBS technique (see the Section 2); bias (the average dc voltage acquired by the r.f. biasing of the sample, see the Section 2); gas mixture and relative flow; film thickness; Ge surface density; total deposition rate of the film; T_{max} : maximum annealing temperature under N₂ flow; film stoichiometry after annealing at 973 K. The target to substrate distance has been fixed at 5 cm for all samples, except for #I and #L fixed at 14 cm. The errors on the N and O values are around 5%.

Sample	Stoichiometry (as-deposited)	Bias (V)	Gas & Flow (sccm)	Thickness (nm)	n_{Ge} (at/cm ²)	V_{dep} (Ge _{at} /s cm ²)	T_{max} (K)	Stoichiometry (after TT)
#A	GeGe ₃ N _{4.6}	0	N ₂ , 40	124	4.3×10^{17}	1.0×10^{15}	923	Ge ₃ N _{2.9} O _{1.3}
#B	GeGe ₃ N _{4.6}	-20	N ₂ , 40	181	6.3×10^{17}	1.0×10^{15}	-	-
#C	Ge ₃ N _{4.2}	-40	N ₂ , 40	141	4.9×10^{17}	1.0×10^{15}	873	Ge ₃ N _{3.5} O _{1.8}
#D	Ge ₃ N _{4.1}	-60	N ₂ , 40	181	6.3×10^{17}	1.0×10^{15}	873	Ge ₃ N _{3.7} O _{0.84}
#E	Ge ₃ N _{4.1}	-80	N ₂ , 40	159	5.5×10^{17}	9.3×10^{14}	873	Ge ₃ N _{3.3} O _{1.6}
#F	Ge ₃ N _{3.7}	-100	N ₂ , 40	160	5.5×10^{17}	8.8×10^{14}	873	Ge ₃ N _{2.8} O _{2.7}
#G	Ge ₃ N _{4.1}	0	N ₂ + Ar, 20 + 20	217	7.5×10^{17}	1.7×10^{15}	973	Ge ₃ N _{4.3} O _{0.10}
#H	Ge ₃ N _{4.1}	0	N ₂ + Ar, 15 + 25	261	9.1×10^{17}	2.0×10^{15}	973	Ge ₃ N _{4.2}
#I	Ge ₂ O _{1.2} N _{1.9}	0	N ₂ + Ar, 20 + 20	127	4.4×10^{17}	1.6×10^{14}	973	Ge ₂ O _{1.3} N _{1.8}
#L	Ge ₂ O _{1.2} N _{1.9}	0	N ₂ + Ar, 20 + 20	43	1.5×10^{17}	1.6×10^{14}	973	-

carried out at 60 W, with a total gas flow of 40 sccm by using pure N₂ or Ar + N₂ gas mixtures (either at 20 + 20 sccm or 25 + 15 sccm of gas flows, respectively) in conjunction with a Ge target (99.999% of purity). The different substrates (silicon, carbon and sapphire) were placed on a sample holder at distances of 5 cm and 14 cm from the target. A set of samples (the so-called biased samples) was biased by a second RF source, which resulted in a mean dc voltage acquired by the layers ranging from 0 V to -100 V. In this way, a controlled ion-bombardment-assisted deposition, at a constant average ion energy, was achieved.

A mass spectrometer, Prisma Plus QMG 220 (Pfeiffer Vacuum), revealed water vapor as the main residual component in the deposition chamber. Parameters chosen for the deposition as well as the resulting film composition are reported in Table 1). A detailed investigation of the as-grown film properties has been reported elsewhere [11].

Investigation of different physical properties upon high temperature annealing required layer deposition on three different substrates, i.e. carbon, silicon and sapphire, during each run. As-deposited films were thermally annealed under N₂ flow (400 sccm) at 873 K, 923 K, 973 K and 1023 K for 1 h, by using a tubular furnace (Lindberg). Before sample annealing, several dry-cleaning vacuum cycles with pure N₂ gas (99.9999%) were done, in order to remove contaminants such as water vapour and CO₂. The heating and cooling ramps were fixed at 90 K/h.

Film stoichiometry was investigated at R.T. by Rutherford Backscattering Spectrometry (RBS), at the scattering angle of 160° on films deposited on carbon substrates by using a 2.0 MeV⁴He⁺ beam (Van de Graaf accelerator at the Laboratori Nazionali di Legnaro). Samples deposited on silicon substrates were characterised by means of glancing x-ray diffraction (XRD) using a Philips diffractometer equipped with glancing-incidence X-ray optics. The analyses were performed at 0.5° of incidence, using CuK_α Ni filtered radiation at 40 kV and 40 mA.

The vibrational dynamics of germanium nitride and oxynitride samples deposited on silicon substrates was probed by Fourier transformed infra-red (FT-IR) spectroscopy measurements. The transmittance spectra of the samples were recorded in the 4000–400 cm⁻¹ range, using a spectrometer Jasco (model FTIR 660 Plus) with a resolution of 4 cm⁻¹. The surface morphology of the samples was investigated by a SEM (Tescan Vega3 XM) equipped with an energy dispersive spectrometry (EDS) detector.

For the characterisation of the electrical conductivity, $\sigma(T)$, films were deposited on sapphire substrates and the measure was carried out at dark in a small furnace operating in vacuum ($P < 10^{-5}$ mbar). Due to the extremely low conductance, S , exhibited by all films, a two coplanar contacts geometry was used, with Au pads sputtered onto the film surface near its borders. Film conductance was measured by electrometers (Keithley either mod. 617 or 6517B) operated in the V/I

mode, i.e. applying a constant bias (typically 50 V) and measuring the current. Particular attention was paid to frequently check the insulation resistance of the whole measuring apparatus. In this respect, an improvement of the insulation resistance of the cables inside the furnace, occurred during the present study, allowed to extend the sensitivity of the measure of more than one order of magnitude. After this upgrade, the low limit of the system sets to $\approx 10^{-15} \Omega^{-1}$ from R.T. to about 600 K, attaining $\approx 10^{-12} \Omega^{-1}$ at 700 K. These values must be considered as the lowest detectable S in our films. As a consequence of this limit in the sensitivity of our apparatus, the real $\sigma(T)$ of several films saturates around R.T. (and in few films until ≈ 450 K) at $\approx 10^{-11} (\Omega \text{ cm})^{-1}$; at $\approx 10^{-9} (\Omega \text{ cm})^{-1}$ for the layers measured before the apparatus upgrade.

Thermal energy in the film was changed very slowly, with a rate of about $0.5 \div 1$ K/min, in cycles from R.T. up to $\approx 600 \div 700$ K and then back to R.T., without any break. Each $S(T)$ curve was collected after T stabilisation to better than 1 K (typically 0.5 K). For every T , 25 \div 30 $S(T)$ values were averaged to calculate the corresponding $\sigma(T)$ value.

It's worthwhile to note that, due to the particular conditions of measure established in this study, all investigated films have undergone a process equivalent to a thermal annealing in vacuum.

3. Results

3.1. Temperature stability of as-deposited films

We have systematically studied high T stability of a-Ge₃N_x and a-Ge₂O_yN_x films measuring in vacuum their electrical behaviour as a function of temperature. Conductivity of as-deposited layers has been measured, during continuous thermal cycles both in the heating, $\sigma_H(T)$, and in the cooling, $\sigma_C(T)$ run. Due to the sensitivity limit of our measuring setup, conductivity has evidenced a saturation (except for #F) at $\approx 10^{-11} (\Omega \text{ cm})^{-1}$, below a T value ranging from 380 K to 460 K, ascribed to the insulation resistance of the apparatus (see the Section 2). For the first cycle, carried out from R.T. to 600 K, we have always found $\sigma_{H1}(T) \geq \sigma_{C1}(T)$ ¹ (Fig. 1) explained with the presence of a conducting layer onto the film surface. For some samples, we further checked that repeating the characterisation up to 600 K, the conductivity measured during the heating overlapped to that of the first cooling run² [12].

During the second cycle, carried out keeping the sample in vacuum and increasing the final T at 700 K, we have observed $\sigma_{H2}(T)$ and $\sigma_{C1}(T)$ overlap up to 600 K (see the Fig. 1). Above 630 K (650 K in some films), $\sigma_{H2}(T)$ branch increases its slope which keeps constant up to 700 K.

¹ The pedix number refers to the cycle number.

² i.e. $\sigma_{Hn}(T) \approx \sigma_{C1}(T)$, with n denoting the n -th thermal cycle ($n > 1$).

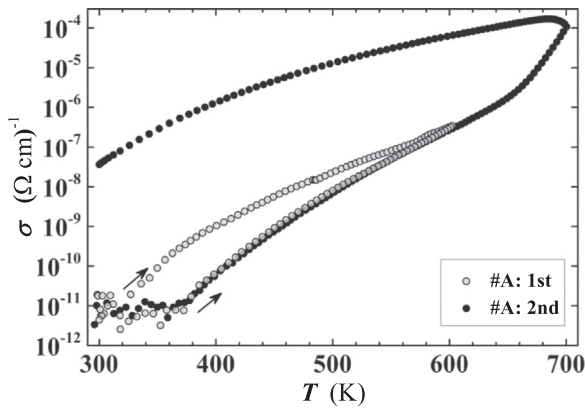


Fig. 1. Temperature dependent conductivity of an unbiased as-deposited a-Ge₃N_x film (#A) upon two consecutive thermal cycles at 600 K (grey circles) and at 700 K (black circles). $\sigma(T)$ branches of the second heating and of the first cooling are perfectly overlapped until 600 K. Below ≈ 380 K, the saturation of $\sigma(T)$ is caused by the sensitivity limit of the measuring apparatus (see the experimental). Arrows indicate the heating branches. Similar behaviour is exhibited by all the other investigated films.

Conductivity measured during the cooling has been $\approx 2 \div 3$ orders of magnitude higher than $\sigma_{H2}(T)$ (Fig. 1). We have always detected $\sigma_{C2}(T) \gg \sigma_{H2}(T)$ in all investigated samples. For instance, for the layer #A at $T = 400$ K, the difference between $\sigma_{H2}(T)$ and $\sigma_{C2}(T)$ is about 4 orders of magnitude (Fig. 1). Additionally, $\sigma_{H2}(T)$ and $\sigma_{C2}(T)$ branches of all films (except for #I) are shifted each other up to ≈ 2 and ≈ 5 orders of magnitude, respectively.

Fig. 2, compares the conductivity of two unbiased a-Ge₃N_x films (#A and #G, see Table 1). Except for the different behaviour at lower T ,³ both $\sigma_{H2}(T)$ branches have similar behaviour, differences being related to the diverse stoichiometry which depends on the gas mixture composition used during film deposition [11]. Conductivity curves of biased films show a similar trend.

A different behaviour is exhibited by quasi-stoichiometric a-Ge₂O_yN_x layers. In fact, in film #I, the $\sigma_{H2}(T)$ slope rises smoothly above 620 K, while $\sigma_{C2}(T)$ and $\sigma_{H2}(T)$ overlap for $670 \text{ K} < T < 700 \text{ K}$. Below ≈ 600 K, $\sigma_{C2}(T)$ and $\sigma_{H2}(T)$ run almost parallel, saturating at $T \lesssim 420$ K.

The conductivity features detected above ≈ 620 K (during the cycle until 700 K) are related to the raise of T only since, up to 600 K, $\sigma_{H2}(T)$ and $\sigma_{C1}(T)$ overlap for all the investigated films. In particular, a value of $630 < T < 650$ K marks the beginning of an irreversible change in the conductivity.

3.2. Thermal annealing in N₂ atmosphere

Film stability has been further studied, investigating layer properties upon high temperature annealing under N₂ flow. Composition, structure and morphology changes have been studied as a function of the annealing T and correlated to the electrical behaviour.

The thermal treatment (TT) under a N₂ flow, has been carried out on a set of pristine as-grown films.⁴ In preliminary tests, we have found that film properties result stable against TT, up to temperatures higher than those found in vacuum (i.e. $630 < T < 650$ K, see Section 3.1). Hence, in a series of trials, we have determined the maximum temperature, T_{max} , reachable by the materials before detecting any sizeable change in their physical properties as composition, microstructure, morphology, etc. Values for T_{max} range from 873 K to 923 K, for biased

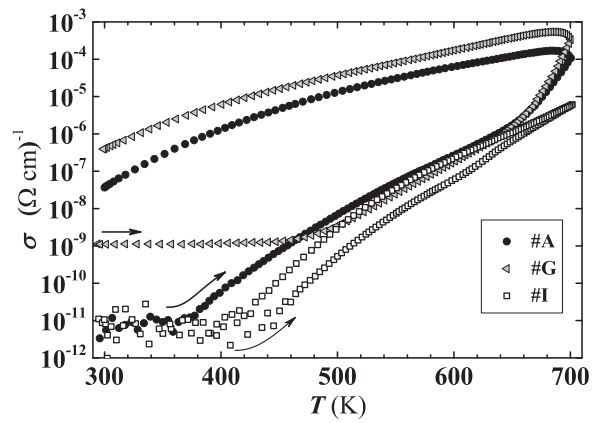


Fig. 2. Conductivity of two unbiased as-deposited a-Ge₃N_x films (#A: $x = 4.6$; #G: $x = 4.1$) and an as-deposited a-Ge₂O_{1.2}N_{1.9} layer (#I), measured during the second thermal cycle (until 700 K). Film #G has been measured before the upgrade of the experimental setup, accounting for the higher saturation value of $\sigma(T)$. In the layer #I the increase of the $\sigma_{H2}(T)$ slope above ≈ 620 appears less marked compared to the other two films. Arrows indicate the $\sigma_{H2}(T)$ branches.

samples, and 973 K for both unbiased and quasi-stoichiometric a-Ge₂O_yN_x layers (see Table 1).

The composition of films, TT at 973 K (last column of Table 1), well explains the meaning of T_{max} : for #A and for biased samples the composition change is evident, with a sizeable decrease of the nitrogen content and the incorporation of oxygen in the films. For #G, #H and #I the composition is very close to the pristine one, even if 973 K represents a high limit value for both #G and #H, as shown by the very small amount of oxygen detected in #G after TT.

The temperature evolution of the film composition, in terms of the relative doses of Ge (Fig. 3), evidences that the Ge content results unaffected by T until 873–923 K, while at 973 K the behaviour is not the same for all the samples.

In detail, in the set biased up to -80 V, we measured a sizeable reduction (from 50% to 70%) of the Ge content, attaining $\approx 90\%$ at -100 V (#F). This decrease can be ascribed to the release of volatile species, whose formation has been favoured by the presence of weak atomic bonds in a defective amorphous lattice. In #F, this condition has been enhanced by both the greatly disordered film structure (the “peening effect” [13,14] i.e. intense ion bombardment due to the high bias) and the understoichiometry [11].

For the biased samples a trend similar to that of Ge is found for the N content (Fig. 4), which keeps constant within 5%, up to 873–923 K. It is noteworthy that the N/Ge atomic ratio does not change in a significant way even if the layers are both overstoichiometric (#B), almost stoichiometric (#D and #E) and understoichiometric (#F), thus revealing the high thermal stability of these films. Increasing T up to 973 K, the decrease of the N content, for the biased set, becomes comparable or even more pronounced than that of Ge, while becomes sizeable the presence of O (see Table 1), whose amount was below the RBS sensitivity in as-deposited layers. Oxygen detected in films is due to germanium oxide formed during and after thermal treatments.

On the contrary, a greater stability against TT has been found in the unbiased samples deposited at high rate in an Ar/N₂ atmosphere (#G and #H). In fact, the Ge dose keeps constant until 973 K, showing a decrease at 1023 K even if still less pronounced than that observed at 973 K in biased layers (Fig. 3). Concerning the N dose, its behaviour at 973 K is similar to the Ge one, but at 1023 K it collapses below the RBS detection limit, resulting in the formation of a Ge film, the O content being below the detection threshold too (Fig. 4).

As regard as films deposited at low rate (#I, Fig. 3), the trend of the Ge dose is similar to that of films #G and #H: at 973 K the decrease is moderate (within 10%) while at 1023 K the lowering is within 25%. A striking difference is found in the case of the N dose, which decreases of

³ The conductivity of the film #G has been measured before the improvement of the insulation resistance of the experimental setup, which explains its higher saturation value at low T .

⁴ This set of samples has been deposited in the same run of that electrically characterised in the Section 3.1.

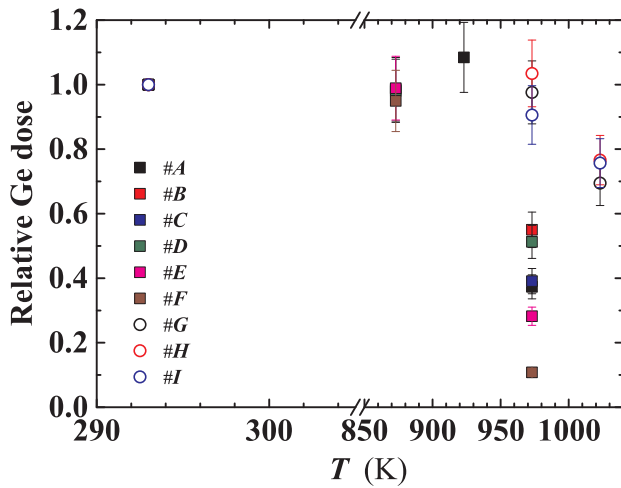


Fig. 3. Relative Ge dose in thermally treated films under a N_2 flow for 1 h at different T . The relative dose has been calculated with respect to the corresponding dose of the as-deposited sample (i.e. before treatment) by RBS technique [11].

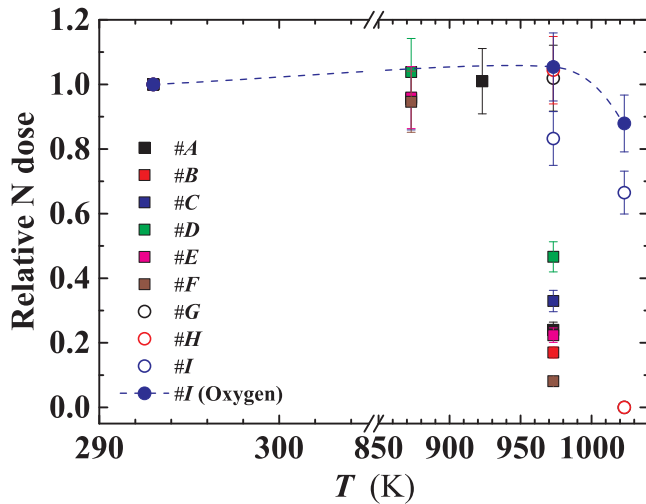


Fig. 4. Relative nitrogen and oxygen (only for film #I) doses in thermally treated films under a N_2 flow for 1 h at different T . Quoted values have been calculated as reported in the Fig. 3.

20% at 973 K but doesn't disappear at 1023 K, still remaining within 60% of the value before TT. Finally, we measured a slight decrease of oxygen content at 1023 K. All these findings allow to conclude that these films, among those studied, are the most stable against TT at high T .

Fig. 5 shows the evolution of XRD spectra following thermal treatments. The spectra point out that all the as-deposited films are very poorly crystallised, independently of the deposition parameters, with only a main band appearing at $20^\circ < 2\theta < 45^\circ$ characterised by the presence of two broad peaks centred at about $2\theta = 25^\circ$ and $2\theta = 35^\circ$. As previously described in the ref. [11], the origin of the main band and of these two peaks can be ascribed to the most intense peaks of c- Ge_3N_4 (α -phase, JCPDS 11–69, and β -phase, JCPDS 38–1374) and c- Ge_2N_2O [15].

After TT, germanium nitride and oxynitride layers keep their amorphicity up to 873 K, independently of their composition (see for example film #F in Fig. 5a). XRD spectra are very similar to those collected in as-deposited layers [11] and do not evidence any new feature emerging from the main amorphous GeN_x band. Raising T to 973 K in the biased samples, we observed a strong decrease of the GeN_x band, completely disappearing in the spectrum of sample #F (Fig. 5a). This outcome is a clear consequence of volatile species effusion from film lattice.

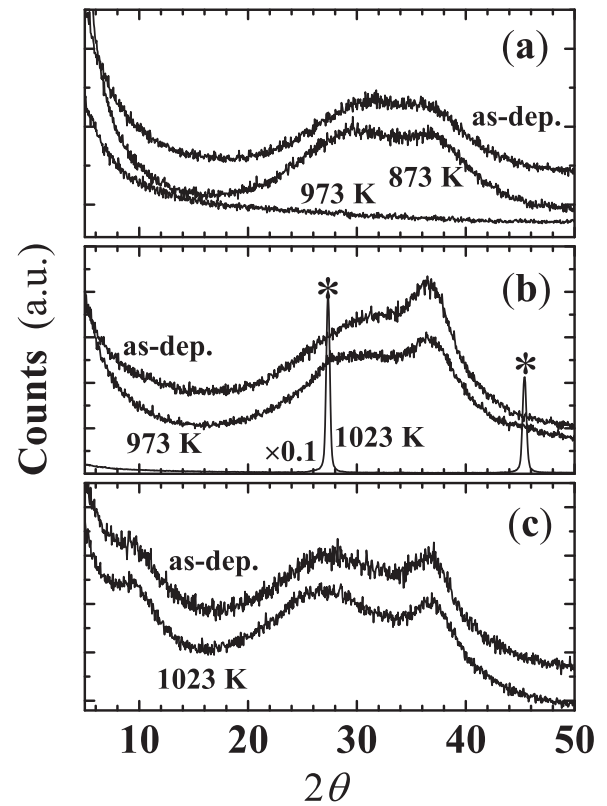


Fig. 5. XRD spectra of samples thermally annealed under a N_2 flow for 1 h, at different temperatures. a) #F as-deposited and after annealing at 873 K and at 973 K; b) #G as-deposited and after TT at 973 K and at 1023 K. Asterisks indicate the peaks of the pure c-Ge phase. c) #I as-deposited and after TT at 1023 K. Spectra of all other investigated samples show features similar to those shown here.

On the other hand, differently from sample #F, spectra of samples #G, #H and #I, do not change after TT at 973 K. Formation of Ge nanocrystallites in the samples #G and #H, due to the N desorption at 1023 K, is highlighted by the appearance of new, narrow peaks ascribed to the pure c-Ge phase (JCPDS 04-0545) and by the disappearance of the GeN_x band (Fig. 5b). It is noteworthy that the spectrum of the layer #I, even at 1023 K presents only minimal changes of the band below $2\theta = 10^\circ$ and a slight change of the shape of the main $Ge_2O_yN_x$ band, with the relative increase of its left part around $2\theta = 25^\circ$ (Fig. 5c). These findings are the result of a partial rearrangement of the film structure occurring during the moderate release of volatile species (see the RBS data).

FTIR analysis of TT samples agrees with XRD results, confirming the absence of any change for biased a- Ge_3N_x samples until 873 K and for the other films until 973 K. Curves reproduced in Fig. 6 are representative of the behaviour observed in all investigated layers. The only variation is a shift of the main Ge-N peak mode towards higher wavenumbers ($10 \div 30 \text{ cm}^{-1}$), which indicates a moderate structural rearrangement with a slight increase of the crystalline order.

At higher T , we detect a drastic decrease of the intensity of the IR features of the biased layers and of those deposited at high rate in Ar/N_2 atmosphere both due to the release of volatile species from film matrix (Fig. 6a). On the contrary, for a- GeO_xN_y layers (sample I) the shift (less than 10 cm^{-1}) and the intensity decrease result moderate even at 1023 K (see Fig. 6b), in agreement with RBS and XRD results.

As far as film morphology is concerned, its evolution at high T is strongly related to the choice of the deposition parameters. For biased samples, the formation of round shaped structures on the film surface is found after TT at 873 K (Fig. 7a). Two types of structures were observed: domes, similar to bubbles, and deep pits, with the formers being predominant in number with respect to the latter. Both structures share an average diameter of few micrometers.

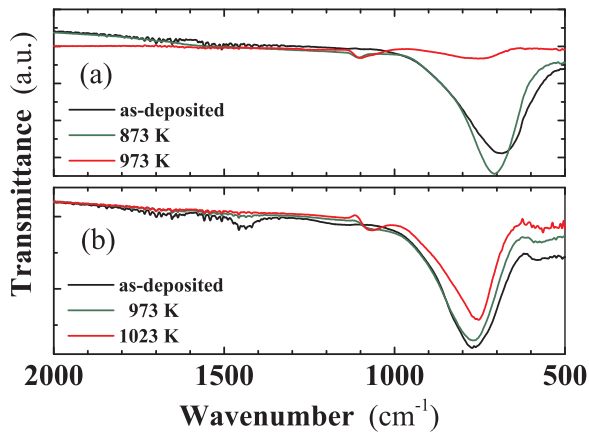


Fig. 6. FT-IR spectra of samples: a) #D (bias: -60 V) as-deposited and after TT at 873 K and 973 K. Similar features have been observed in all but $\text{Ge}_2\text{O}_{1.2}\text{N}_{1.9}$ films. b) #I as-deposited and after treatment at 973 K and 1023 K.

EDS analysis has revealed that the pit depth reaches the film-Si substrate interface. A further heating until 973 K causes a complete disappearance of the domes, leaving only some residual pits. In some cases, a rough morphology appears together with the residual pits. These findings, combined with the RBS analysis, clearly indicate that heating gives rise to the aggregation of volatile species in gas bubbles, which trying to escape from the film matrix lift up locally the film, then forming domes at the surface. Deep pits, in the film annealed at higher T , are the result of gas molecules effusion from the surface. On the contrary, neither domes nor pits have been observed in the unbiased layers, whose morphology has resulted completely unaffected until 973 K. Raising the annealing T at 1023 K, morphology of #I has not yet exhibited any change (Fig. 7b), while a rough morphology has appeared for #G and #H (Fig. 7c), which may be related to the formation of c-Ge domains, as found by XRD analysis.

Conductivity of films representative of the different groups, has been measured after the TT under the N_2 flow. To allow a reliable comparison between as-deposited and TT films, hereafter only the $\sigma_{C1}(T)$ branch will be taken into account. We found that the electrical behaviour of TT a- Ge_3N_x ($3.7 < x < 4.6$) and a- $\text{Ge}_2\text{O}_y\text{N}_x$ films mainly depends on their composition and to a minor extent on the deposition parameters.

The $\sigma_{C1}(T)$ curves for the investigated samples are reproduced in Figure ((8)-c). During the characterisation we faced technical problems which have caused a reduction of the T range of measure for as-deposited #L (Fig. 8c) and prevented to reach $T > 530$ K for as-deposited #H and TT #L (Figs. 8b and 8c, respectively). For as-deposited #B and #G, the conductivity has been measured before experimental setup upgrade, explaining the reduced range of T values.

We have found in all TT layers an upward shift within one order of magnitude of the $\sigma_{C1}(T)$ curve, with respect to that measured in as-deposited. This shift can be considered relatively small if compared to the whole range of conductivity change with T (several orders of magnitude) exhibited by this class of materials, suggesting a good film stability against thermal treatment under N_2 flow, even at annealing T as high as 973 K.

In detail, in overstoichiometric a- $\text{GeGe}_3\text{N}_{4.6}$ samples (#A and #B) both as-deposited and TT curves are partially overlapped tough in two distinct T regions (Fig. 8a). This outcome was in part expected, since the two as-deposited films have the same composition, apart for the small bias (-20 V) applied to #B. We expect that TT at 873 K favouring a partial rearrangement of the film matrix could have contributed to reduce the difference in their conductivity.

Considering the almost stoichiometric a- $\text{Ge}_3\text{N}_{4.1}$ layers (#G and #H) deposited at high rate, $\sigma_{C1}(T)$ curves of as-deposited films appear to share a similar behaviour and a partial overlapping for $500 < T < 530$ K

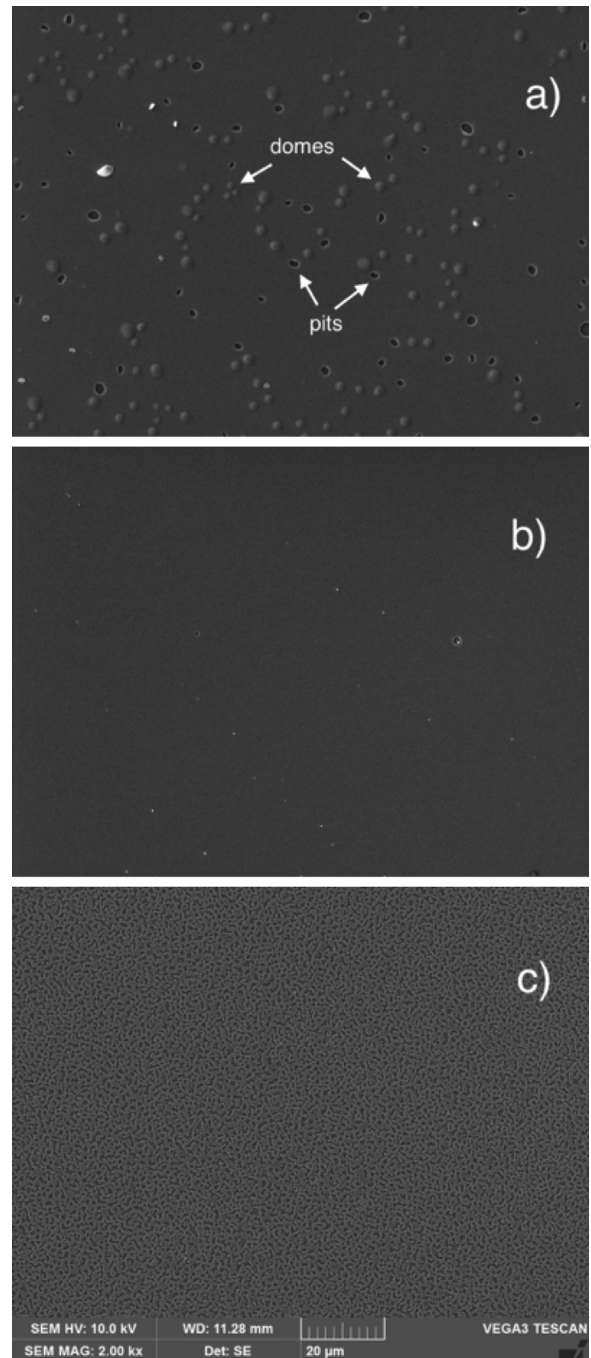


Fig. 7. SEM images of films surface, after 1 h of annealing in N_2 , at different T : a) #D @ 873 K; b) sample #I @1003 K; c) sample #G @1023 K. In all images, the scale bar is as reported in the panel c).

(Fig. 8b). After TT, the $\sigma_{C1}(T)$ of both films overlap for $400 \lesssim T \lesssim 430$ K, then running almost parallel for $T > 530$ K. As for the previous case, the conductivity appears to be more tightly related to the film composition, showing only a minor dependence on the deposition parameters (i.e. precursor gas mixture, see Table 1).

Finally, we detected a sizeable difference in the conductivity of the two a- $\text{Ge}_2\text{O}_{1.2}\text{N}_{1.9}$ layers having the same nominal composition but very different thickness (#I and #L, see Table 1). Except at the lowest T , both $\sigma_{C1}(T)$ curves of the thinner film #L are shifted to higher values (Fig. 8c). This finding can be explained supposing an intrinsic higher film defectivity due to its reduced thickness [12]. Compared to all other investigated films, #I has evidenced the highest upward shift of the TT $\sigma_{C1}(T)$ curve, more evident at the lowest T . This finding suggests a

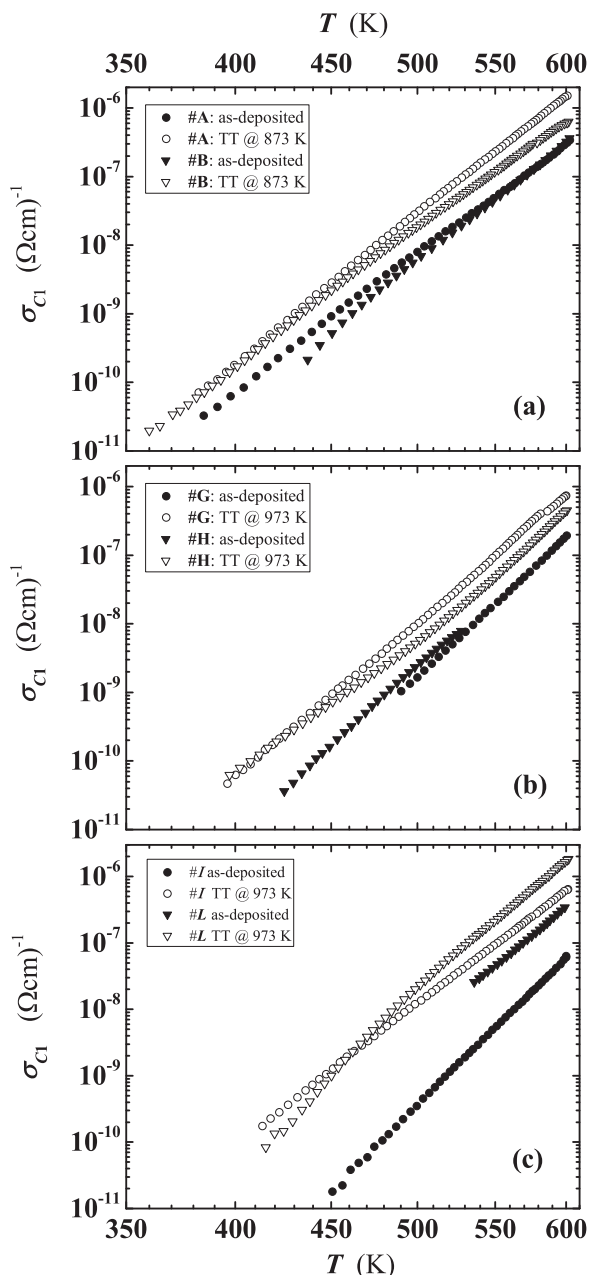


Fig. 8. Temperature dependence of the conductivity measured during the first cooling run in as-deposited films and in those TT in N_2 atmosphere at $T \leq T_{max}$ for 1 h. (a) $a\text{-Ge}_3\text{N}_{4.6}$ films deposited under high rate, without (#A) and with a low applied bias (#B: -20 V). (b) Quasi-stoichiometric $a\text{-Ge}_3\text{N}_{4.1}$ films deposited without any applied bias, at two different Ar + N_2 gas mixture (Table 1). (c) $a\text{-Ge}_2\text{O}_{1.2}\text{N}_{1.9}$ films. For some samples (e.g. as-deposited #B and #G) the reduced T range for the measured conductivity is due to the sensitivity limit of the experimental setup or to technical problems occurred during measurement (for details see the text, Section 3.2).

stronger dependence of the electrical properties on the annealing T , in countertrend with conclusions derived by the analysis of the other properties claiming, instead, a good film stability until 973 K.

4. Discussion

The analysis of experimental results has clearly evidenced that physical properties of $a\text{-Ge}_3\text{N}_x$ and $a\text{-Ge}_2\text{O}_y\text{N}_x$ can be changed by thermal annealing.

All as-deposited films result amorphous [11] and thermal treatment under N_2 flow at T_{max} ($873 \leq T_{max} \leq 973$ K) do not recrystallise the layer

matrix (see Fig. 5). We have found that TT at 1023 K (i.e. at $T > T_{max}$) causes minor changes in the shape of the XRD spectra of $a\text{-Ge}_2\text{O}_y\text{N}_x$ films, but the appearance of intense Ge peaks in stoichiometric $a\text{-Ge}_3\text{N}_{4.1}$ layers and the disappearance of the main Ge_3N_4 amorphous band in biased films. These outcomes are related to N effusion, due to breaking of N and Ge bonds at high T , that will cause a rearrangement of the film matrix. The disappearing of the Ge-N related vibrational mode from the IR spectrum, after annealing above T_{max} supports the hypothesis of a lattice reorder.

Tough the amorphous structure of films results relatively stable against TT, below or close to T_{max} , other types of changes have been detected depending on the layer properties (e.g. composition, deposition conditions, etc.). Surface defects, such as domes and pits, start to form at 873 K in biased $a\text{-Ge}_3\text{N}_x$ samples and, at T higher than 973 K, in the unbiased ones. $a\text{-Ge}_2\text{O}_y\text{N}_x$ films appear to be more stable even at T as high as 1023 K [16,17]. Formation of domes and pits is compatible with the release of N-based volatile species from the film, in agreement with the RBS analysis. This phenomenon is expected to increase the defect density inside the layer leaving broken and/or unsaturated bonds.

Appearance of Ge nanocrystallites, observed in films deposited at high rate in Ar + N_2 atmosphere (#G and #H) can be explained with an enhanced N effusion (rather than Ge), occurring at 1023 K. In fact, a sizeable release of nitrogen is expected to occur during TT above 973 K (823 K for $a\text{-Ge}_3\text{N}_4$ annealed in vacuum, as experimentally shown by Wang et al. [16]) inducing Ge segregation and a melting process around 1023 K [18]. This mechanism is at the base of the nano-crystallisation of a-Ge observed in these films (see Fig. 5b).

The electrical characterisation carried out after the thermal treatment in N_2 atmosphere at T_{max} (i.e. before N desorption), reveals a moderate increase of the conductivity in all films except in #I. This increase, can be explained with the nucleation of several defects caused by the effusion of weakly-bonded species during TT. In the case of the sample #I, the presence of oxygen in the film matrix, preferentially bonded to Ge, can induce the nucleation of additional defects upon annealing at high T [12,19], leading to a further raise of the $\sigma_{C1}(T)$ curve.

As regards the conductivity of as-deposited $a\text{-Ge}_3\text{N}_x$ and $a\text{-Ge}_2\text{O}_y\text{N}_x$ films, our findings are in agreement with results of Kutsuki et al. and Maeda et al. who reported, for Ge_3N_x films heated in vacuum, reduction of GeO_2 to volatile GeO [18,17,20]. Maeda et al. found that the GeO evaporation sets-in at $T_{des} \approx 673$ K, value close to the threshold detected in our experiments carried out by using a technique (conductivity) different (also in terms of sensitivity) from that reported in the ref. [18].

Although a specific investigation about the GeO evaporation effects on the electrical properties is still missing in literature, we can reasonably assert that conductivity changes above $\approx 630 \div 650$ K, detected in as-deposited films, are related to oxygen desorption from the film surface. The surface will be involved also in the conduction process, after the oxide desorption, contributing to modify the measured conductivity. Formation of additional defects, upon GeO evaporation, cannot be excluded, favouring the reduction of the insulating properties of films. This reduction is expected to be more effective in $a\text{-Ge}_2\text{O}_y\text{N}_x$ due to the presence of oxygen throughout the film matrix.

Oxygen based molecules can be considered directly and/or indirectly responsible of the conductivity change observed during the measurements. In fact, an oxide layer, few nanometers thick, is formed on film surface [18]. During heating at $T \geq 650$ K, oxygen, preferentially bound to Ge [19], will start to evaporate as GeO molecules, inducing the formation of a high concentration of defects as germanium dangling-bonds, Ge_{DB} , and nitrogen dangling-bonds, N_{DB} at the surface. The resultant increase of the density of states (DOS) inside the material band-gap (band tails and mid-gap states) can account for the conductivity raise (see the Figs. 1 and Figs. 2).

GeO evaporation from the film surface takes place also in as-deposited $a\text{-Ge}_2\text{O}_{1.2}\text{N}_{1.9}$ layers, tough to a lower extent below ≈ 630 K, especially for the sample #I. In fact, the Ge-O bonds formed during film

deposition make the layer matrix more stable against high T annealing, compared to the oxide formed on the surface of a-Ge₃N_x films upon exposition to ambient air. Anyway, this process seems to be effective only for thicker a-Ge₂O_yN_x film (i.e. for $\#l$) since for the thinner film $\#L$, we measured conductivity values more similar to those detected in a-Ge₃N_x films. The lower insulation of $\#L$ is probably related to a higher intrinsic structural disorder due to very reduced thickness (see Table 1) [12]. Indeed, disorder in amorphous materials induces a large density of dangling bonds in the matrix (lower bonding coordination numbers) resulting in an easier desorption of GeO_x molecules.

GeO evaporation is expected to be enhanced in a-Ge₃N_x (as experimentally observed) with respect to a-Ge₂O_yN_x layers, since in the formers the surface GeO group is bound only to N back atoms (O-Ge-N), while in the latter GeO can be bound with O atoms of the film matrix below, as O-Ge-O bonds. It is important to emphasise that inside the a-Ge₂O_yN_x matrix, oxygen and nitrogen are both bound to Ge but not each other [19]. N atoms, being less electronegative than O, can form less stable bonds at the surface of a-Ge₃N_x layers.

Our experimental work clearly demonstrates the strong sensitivity of the electrical characterisation to detect changes of physical properties upon annealing in vacuum [21–23]. In particular, conductivity measured as a function of T allows to monitor the change when it is occurring [21,22].

From a technological point of view, the excellent insulation properties detected in our a-Ge₃N_x and a-Ge₂O_yN_x layers, against TT at high temperature under N₂ flow (Fig. 8), make these materials ideal candidates for the fabrication of different kind of device [2,5,9,11].

Finally, we desire to comment about the upward shift of the conductivity curves of heated layers up to 700 K, in high vacuum. We have also explored an alternative explanation for the observed behaviour, carrying out a SEM micro-analysis to reveal Au⁵⁺ diffusion inside the film matrix, accounting for a possible increase of the conductivity. Neither gold diffusion nor Au based Ge alloy formation has been detected by EDS analysis. This finding support the hypothesis of a conductivity change related to the change of structural defects density.

5. Conclusions

The effects of thermal treatments on the physical properties of germanium nitride and oxynitride films have been investigated in detail. This study has evidenced that the conductivity of a-Ge₃N_x ($3.7 < x < 4.6$) and of quasi-stoichiometric a-Ge₂O_yN_x thin films exhibits an irreversible change at $T \gtrsim 630$ K detected during measurement in high vacuum. Above this temperature, $\sigma(T)$ exhibits an hysteresis, with features depending on the film composition and the annealing conditions. Irreversibility in $\sigma(T)$ has been explained as the reduction of native GeO₂ into volatile GeO, considering that the latter occurs in vacuum at a temperature close to the threshold of irreversibility detected in our films.

Analysis of film properties, thermally annealed in N₂, has revealed an improved stability up to 973 K, with formation of domes and pits on film surface at higher T originated by the effusion of volatile N-based molecules from the film matrix. Ge nano-crystallisation has been detected in a-Ge₃N_x films, upon TT in N₂ around 1023 K.

The knowledge gained by the study of the irreversible process occurring in the investigated class of materials has allowed to identify the material and the deposition/process conditions to get an optimal passivating layer for the fabrication of several devices such as HPGe detectors. The best candidate to cover this role has been found to be a quasi-stoichiometric a-Ge₂O_yN_x film of ≈ 130 nm of thickness.

Finally, we have demonstrated that $\sigma(T)$, at least in this class of materials, is capable to monitor temperature dependent changes in the physical properties of a thin film, occurring during the measurement. This feature is generally prevented to other investigation techniques, either for practical reasons or for their intrinsic limits. In this respect,

$\sigma(T)$ results a powerful and straightforward tool to characterise the behaviour of dielectric layers.

References

- [1] H. Watanabe, K. Kutsuki, A. Kasuya, I. Hideshima, G. Okamoto, S. Saito, T. Ono, T. Hosoi, T. Shimura, Gate stack technology for advanced high-mobility Ge-channel metal-oxide-semiconductor devices – fundamental aspects of germanium oxides and application of plasma nitridation technique for fabrication of scalable oxynitride dielectrics, *Curr. Appl. Phys.* 12 (2012) S10–S19, <http://dx.doi.org/10.1063/1.4826142>.
- [2] G.M. Wu, C.K. Yang, H.C. Lu, T.W. Chang, Plasma enhanced germanium nitride dielectric thin films for phase-change recording systems, *Vacuum* 83 (2009) S33–S35.
- [3] K. Prabhakaran, T. Ogino, Oxidation of Ge(100) and Ge(111) surfaces: an UPS and XPS study, *Surf. Sci.* 325 (1995) 263–271, <http://dx.doi.org/10.1016/j.matchemphys.2015.05.022>.
- [4] J.S. Hovis, R.J. Hamers, C.M. Greenleaf, Preparation of clean and atomically flat germanium(001) surfaces, *Surf. Sci.* 440 (1999) L815–L819, <http://dx.doi.org/10.1016/j.matchemphys.2015.05.022>.
- [5] Z. Xu, L. Bo, P. Cheng, R. Feng, Z. Xi-Lin, S. San-Nian, W. Liang-Yong, C. Yan, W. Liang-Cai, Y. Dong-Ning, S. Zhi-Tang, F. Song-Lin, Germanium nitride as a buffer layer for phase change memory, *Chin. Phys. Lett.* 29 (2012) 107201, <http://dx.doi.org/10.1088/0256-307X/29/10/107201>.
- [6] P. Bhatt, K. Chaudhuri, S. Kothari, A. Nainani, S. Lodha, Germanium oxynitride gate interlayer dielectric formed on Ge(100) using decoupled plasma nitridation, *Appl. Phys. Lett.* 103 (17) (2013) 172107, <http://dx.doi.org/10.1063/1.4826142>.
- [7] H. Zhao, H.-S. Kim, F. Zhu, M. Zhang, I. OK, S.I. Park, J.H. Yum, J.C. Lee, Metal-oxide-semiconductor capacitors on GaAs with germanium nitride passivation layer, *Appl. Phys. Lett.* 91 (17) (2007) 172101, <http://dx.doi.org/10.1063/1.2795802>.
- [8] T. Yashiro, Some properties of vapor deposited Ge₃N₄ films and the Ge₃N₄ Ge interface, *J. Electrochem. Soc.* 119 (6) (1972) 780–783, <http://dx.doi.org/10.1149/1.2404328>.
- [9] S. Carturan, G. Maggioni, S.J. Rezvani, R. Gunnella, N. Pinto, M. Gelain, D.R. Napoli, Wet chemical treatments of high purity Ge crystals for g-ray detectors: surface structure, passivation capabilities and air stability, *Mater. Chem. Phys.* 161 (2015) 116–122, <http://dx.doi.org/10.1016/j.matchemphys.2015.05.022>.
- [10] I. Chambouleyron, A.R. Zanatta, Nitrogen in germanium, *J. Appl. Phys.* 84 (1) (1998) 1, <http://dx.doi.org/10.1063/1.368612>.
- [11] G. Maggioni, S. Carturan, L. Fiorese, N. Pinto, F. Caproli, D.R. Napoli, M. Giarola, G. Mariotto, Germanium nitride and oxynitride films for surface passivation of Ge radiation detectors, *Appl. Surf. Sci.* 393 (2017) 119–126, <http://dx.doi.org/10.1016/j.apsusc.2016.10.006>.
- [12] N. Pinto, F. Caproli, G. Maggioni, S. Carturan, D.R. Napoli, The Meyer-Neldel rule in the conductivity of insulating germanium nitride and oxynitride films, *J. Non-Cryst. Sol.* 452 (2016) 280–285, <http://dx.doi.org/10.1016/j.jnoncrysol.2016.09.006>.
- [13] A. Fourrier, A. Bosseboeuf, G. Gautherin, Annealing effect on mechanical stress in reactive ion-beam sputter-deposited silicon nitride films, *Jpn. J. Appl. Phys.* 30 (7) (1991) 1469–1474.
- [14] M.Y. Chen, D. Li, X. Lin, V.P. Dravid, Y.-W. Chung, M.-S. Wong, W.D. Sproul, Analytical electron microscopy and Raman spectroscopy studies of carbon nitride thin films, *J. Vac. Sci. Technol. A* 11 (3) (1993) 521–524, <http://dx.doi.org/10.1116/1.578765>.
- [15] J.D. Jorgensen, S.R. Srinivasa, G. Labbe, J.C. Roullet, Time of flight neutron diffraction study of germanium nitride oxide, Ge₂N₂O, *Acta Cryst. B* 35 (1979) 141–142, <http://dx.doi.org/10.1107/S0567740879002752>.
- [16] S.J. Wang, J.W. Chai, J.S. Pan, A.C.H. Huan, Thermal stability and band alignments for Ge₃N₄ dielectrics on Ge, *Appl. Phys. Lett.* 89 (2006) 022105, <http://dx.doi.org/10.1063/1.2220531>.
- [17] K. Kutsuki, I. Hideshima, G. Okamoto, T. Hosoi, T. Shimura, H. Watanabe, Thermal robustness and improved electrical properties of ultrathin germanium oxynitride gate dielectric, *Jpn. J. Appl. Phys.* 50 (2011) 010106, <http://dx.doi.org/10.1143/JJAP.50.010106>.
- [18] T. Maeda, T. Yasuda, M. Nishizawa, N. Miyata, Y. Morita, S. Takagi, Pure germanium nitride formation by atomic nitrogen radicals for application to Ge metal-insulator-semiconductor structures, *J. Appl. Phys.* 100 (2006) 014101, <http://dx.doi.org/10.1063/1.2206395>.
- [19] D.J. Hymes, J. Rosenberg, Growth and materials characterization of native germanium oxynitride thin films on germanium, *J. Electrochem. Soc.* 135 (1988) 961–965, <http://dx.doi.org/10.1149/1.2095851>.
- [20] K. Prabhakaran, F. Maeda, Y. Watanabe, T. Ogino, Distinctly different thermal decomposition pathways of ultrathin oxide layer on Ge and Si surfaces, *Appl. Phys. Lett.* 76 (2000) 2244, <http://dx.doi.org/10.1063/1.126309>.
- [21] R. Murri, N. Pinto, G. Ambrosone, U. Coscia, Electrical resistivity of a-SiC:H as a function of temperature: evidence for discontinuities, *Phys. Rev. B* 62 (2000) 1801–1805, <http://dx.doi.org/10.1103/PhysRevB.62.1801>.
- [22] R. Murri, N. Pinto, S. Giuliadori, G. Ambrosone, U. Coscia, Reversible effects in electrical conductivity of a-SiC:H, *J. Mater. Sci. - Mater. El* 14 (2003) 341–344.
- [23] N. Pinto, M. Ficcidenti, L. Morresi, G. Ambrosone, U. Coscia, R. Murri, Electrical transport properties of microcrystalline silicon grown by PECVD, *J. Appl. Phys.* 96 (2004) 7306–7311, <http://dx.doi.org/10.1063/1.1812818>.